Dry deposition of ammonia in a coastal dune area: Measurements and modeling

K.J.A. Vendel [a],[*], R.J. Wichink Kruit [a], M. Blom [b], P. van den Bulk [b], B. van Egmond [b], A. Frumau [b], S. Rutledge-Jonker [a], A. Hensen [b], M.C. van Zanten [a],[c]

[a] *National Institute for Public Health and the Environment (RIVM), P.O. Box 1, 3720 BA, Bilthoven, the Netherlands*
[b] *Netherlands Organisation for Applied Scientific Research (TNO), P.O. Box 15, 1755 ZG, Petten, the Netherlands*
[c] *Wageningen University & Research (WUR), P.O. Box 47, 6700 AA, Wageningen, the Netherlands*

HIGHLIGHTS

- Dry deposition fluxes of ammonia were measured in a Dutch coastal dune area.
- Half-hourly data were collected for a full year with a wet denuder instrument.
- Fluxes from the aerodynamic flux-gradient method were compared with modeling.
- Modeled fluxes captured measured diurnal variations, but overestimated deposition.
- Modeled fluxes were sensitive to leaf area index and compensation points.

ARTICLE INFO

ABSTRACT

Ammonia deposition is a threat to many natural ecosystems, including coastal dune areas, because of eutrophication and acidification. Direct measurements of ammonia fluxes are nevertheless scarce. In this paper we present a full year of measurements to derive the ammonia dry deposition flux in a Dutch coastal dune ecosystem, based on the aerodynamic flux-gradient method (AGM). We found a mean ammonia flux of -7.1 ± 1.7 ng m^{-2} s^{-1}, and an annual ammonia deposition flux of -132 ± 32 mol ha^{-1} yr^{-1} (equivalent to 1.8 ± 0.4 kg N ha^{-1} yr^{-1}), which is at the low end of the range from estimates from literature made with inferential methods. Modeling the fluxes with the DEPAC module resulted in a mean flux of -17.0 ng m^{-2} s^{-1}. The model overestimated the deposition fluxes, but diurnal variations of the fluxes derived from measurements were well captured by the model. We propose to change certain DEPAC parameters, like the leaf area index, to values more applicable for a dune ecosystem and show that this improves the agreement between model and measurements.

1. Introduction

The majority of the Dutch North Sea coast consists of coastal sand dunes, hereby representing a substantial part of the total European dune area. Such sand dunes are a unique ecosystem with a large diversity of species, characterized by dry soil with low nutrient availability. As such, the dune ecosystem represents an important habitat type within the Natura 2000 network. However, keeping the dunes in good natural condition and preserving the unique habitat types is rather a challenge. One of the major threats to dune ecosystems is nitrogen deposition, leading to a loss of biodiversity, a decline of the typical dune ecosystem

and even disappearance of certain rare species (Aggenbach et al., 2017; Bobbink et al., 2010; Field et al., 2014; Ford et al., 2016; Kooijman et al., 2021; Phoenix et al., 2012). To prevent this, measures are needed for conservation and restoration of dune areas, but also for reduction of nitrogen deposition. For this, a better understanding of the processes of nitrogen deposition is needed, not only in dunes but also in other ecosystems. In the Netherlands, ammonia has the largest contribution to the total nitrogen deposition, and therefore the focus is on this compound.

Up to now, annual nitrogen deposition estimates in dune ecosystems were made by the inferential method (e.g. Flechard et al. (2011)). The nitrogen deposition assessed with this method usually includes reduced
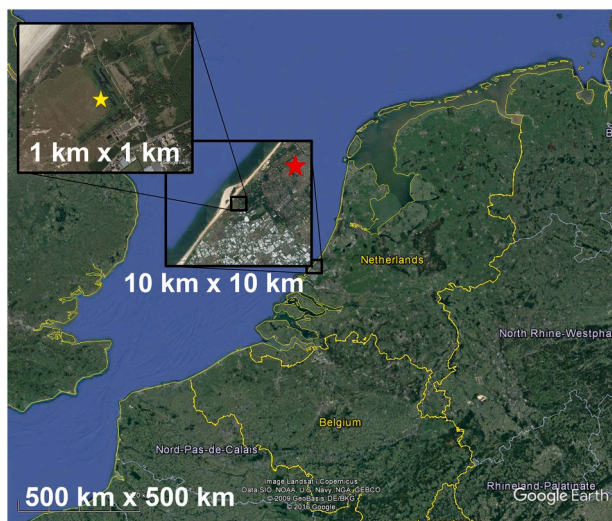

Fig. 1. Location of the measurement site in dune area Solleveld. The location of The Hague is marked with a red star in the 10 × 10 km inset, and the location of the GRAHAM instrument with a yellow star in the 1 × 1 km inset.

(NH$_x$) and oxidized (NO$_x$) nitrogen, as well as wet and dry deposition. The reported numbers range between 3 and 30 kg N ha^{-1} yr^{-1} for various European sand dune areas (Field et al., 2014; Jones et al., 2004; Kooijman et al., 2017; Remke, 2009). The uncertainty on this type of inferential flux estimations is large, due to uncertainty in the derivation of the deposition velocities. The Eddy Covariance (EC), Relaxed Eddy Accumulation (REA) or the aerodynamic flux-gradient method (AGM) are potentially more accurate methods to measure ammonia fluxes, but these are challenging for ammonia because of technical difficulties to measure ammonia with high enough time resolution.

Because detailed knowledge about deposition in coastal dune areas is scarce, a measurement campaign was set up in dune area Solleveld (Netherlands). Half-hourly data of dry ammonia fluxes were obtained during one year using the aerodynamic flux-gradient method (AGM). This method is commonly used when EC techniques for flux measurements are not readily available (Erisman and Wyers, 1993; Nemitz et al., 2004; Trebs et al., 2021; Wyers et al., 1993). The main objectives of this study were how large the actual dry deposition flux of ammonia was in Solleveld and how well it could be modeled by the dry deposition module, DEPAC (DEPosition of Acidifying Components). To gain a better understanding of the exchange processes in Solleveld, the AGM derived fluxes were analyzed for different circumstances (e.g. season and wind direction). Furthermore, we evaluated the DEPAC module for this dune area, while dunes are not separately parametrized as a land use class in DEPAC. Based on the comparison of measured and modeled fluxes, we suggest some DEPAC parameters which could be optimized to improve the DEPAC parametrization for dunes.

2. Materials and methods

2.1. Experimental site and setup

From September 2014 to September 2015 flux-gradient measurements of ammonia were made in Solleveld (52°2′49.22″N, 4°11′56.82″E). This Natura 2000 area is a narrow strip of land to the southwest of The Hague in the Netherlands (Fig. 1), mainly consisting of grey dunes (habitattype H2130). To the southwest of the measurement site predominantly sand sedge (Carex arenaria), moss and lichen are growing, giving a fetch of several hundreds of meters in the prevailing wind direction. To the northeast, the site is flanked by reed growing on the edge of a nearby infiltration pond.

The GRadient Ammonia High Accuracy Monitor (GRAHAM) was

used for the ammonia concentration gradient measurements. This instrument measured ammonia concentrations at three different heights (3.6, 1.7 and 0.8 m) with an annular denuder system which is connected to a detector unit. The GRAHAM is an advanced version of the AMANDA instrument, which is described in more detail by Wyers et al. (1993). The GRAHAM is suited for gradient measurements due to its low detection limit (0.1 μg/m^3), high precision (1.9%) and high time resolution (10 min, which is averaged to a 30 min mean). A detailed description of the GRAHAM equipment and the measurement technique are given by Wichink Kruit et al. (2007). A 3D sonic anemometer (Windmaster pro, Gill) mounted at a height of 5.15 m measured meteorological variables such as wind direction and wind speed, from which friction velocity (u_*), sensible heat flux (H) and Obukhov length (L) were derived.

2.2. Derivation of the fluxes

Exchange fluxes of ammonia were derived using the aerodynamic gradient or flux-profile technique. We used the following equation to relate the flux of ammonia to the vertical ammonia gradient:

$$F_\chi = -u_* C_* = -ku_* \frac{\left[\chi(z) - \chi(z_{0\chi})\right]}{\left[\ln\left(\frac{z}{z_{0\chi}}\right) - \Psi_\chi\left(\frac{z}{L}\right) + \Psi_\chi\left(\frac{z_{0\chi}}{L}\right)\right]} \qquad (1)$$

Where k is the von Karman's constant ($k = 0.4$), χ the ammonia concentration, z the height above the displacement height d (defined by 2/3 of the canopy height, which is 0.1 m for Solleveld), $z_{0\chi}$ the characteristic length scale of the underlying surface for ammonia and $\Psi_\chi(\zeta)$ the integrated stability function for ammonia. For the latter we used the functions of Dyer (1974) and Paulson (1970) for unstable conditions (i.e. $z/L < 0$) and of Beljaars and Holtslag (1991) for stable conditions (i.e. $z/L > 0$). The flux-profile technique assumes horizontal homogeneous conditions and no flux divergence (e.g. by non-stationary conditions or chemical reactions). Because the GRAHAM measured ammonia concentrations at three heights, the quotient in Eq. (1) was calculated by linear regression through the measured concentrations and the stability corrected heights. More details on the method can be found in Wichink Kruit et al. (2007).

2.3. Data set description

We measured ammonia concentrations with the GRAHAM every 10 min for one year, but with several gaps. Between October 26 and November 13, data loss occurred due to instrument failure. At the end of 2014 the GRAHAM was turned off due to freezing temperatures and the measurement campaign was suspended for the whole month of January 2015. At the beginning of February, the campaign was restarted but winter weather and instrument failure caused various gaps in the dataset until March 3. On July 25 a summer storm damaged the site resulting in a loss of data for almost three weeks. Smaller gaps in the data were caused by calibration periods (2 h every other day) and short term instrumental errors. In addition to missing data, part of the data was filtered out based on instrumental quality checks to assure data quality. The remaining valid 10 min ammonia concentrations were averaged to half-hourly data for each of the three heights, and used to calculate half-hourly fluxes with Eq. (1). Next, quality checks on the data were performed, i.e. whether calculated ammonia concentrations at $z = z_0$ was larger than zero, whether the calculated reference concentration at 1 m (using the linear regression through the measured concentrations and corresponding stability corrected heights to calculate the concentration at 1 m) was higher than the level of detection and whether the wind was not coming from behind the measurement box (winddirections between 100° and 120° were filtered out). Such quality checks ensure that the criteria of the flux-gradient method are met. No stationarity test was performed originally. When this was added in the review process the outcome was an additional rejection of 3% of the data, altering the mean
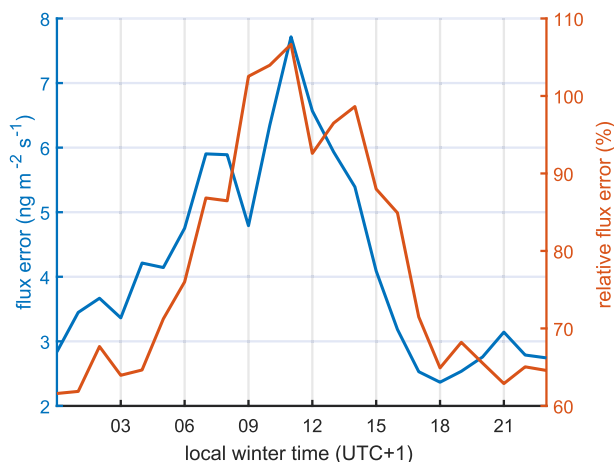
Fig. 2. Diurnal variation of the absolute (blue) and relative (red) random errors on the ammonia fluxes in Solleveld.

flux by 0.3%. Due to this small influence this correction has not been implemented in the data analysis presented in this article.

Between June 30 and July 17 in 2015 we observed a few days with unexplainable high emission fluxes during a heatwave, while concentrations were not notably different from the rest of the year. In Supplementary Sec. 6.1 we discuss possible causes for these large ammonia emissions and our reasons to exclude this period from the analysis. Finally, we filtered out all data with a friction velocity u_* below 0.1 m/s. Lower u_* indicate low turbulence conditions, in which case large gradients could be measured while actual fluxes are small due to limited mixing. Considering all gaps in the data and filtering, we were left with 28% data coverage for the half-hourly ammonia fluxes between September 2014 and September 2015. The data coverage was similar for day and night, but the majority of missing data occurred in winter, when on average more precipitation and lower temperatures occur.

To find out if concentration data of two (instead of three) heights sufficed to derive fluxes, we selected a subset of the data for which concentrations at all three heights were available. Within this subset, we calculated the mean flux using ammonia concentrations at all three measurement heights. Next, we calculated mean fluxes using permutations of two of the three measurement heights. Using concentrations of the high and low measurement height gives a mean flux only 0.1% different from the mean flux derived with three measurement heights. Using the high and middle denuders only, an overestimation of 1.5 ng m^{-2} s^{-1} (around 20%) of the mean flux is calculated, while using the middle and low denuders leads to an underestimation of similar magnitude (1.4 ng m^{-2} s^{-1}, or 19%). Based on these results, fluxes presented in this article were only derived when concentrations of at least the lowest and highest measurement height were available.

2.4. Error analysis

The relative random error in our flux calculation (equation 3) is given as:

$$\frac{\delta F_\chi}{|F_\chi|} = \sqrt{\left(\frac{\delta u_*}{|u_*|}\right)^2 + \left(\frac{\delta C_*}{|C_*|}\right)^2} \tag{5}$$

The relative random error in the friction velocity was determined to be 10% (Finkelstein and Sims, 2001). The relative random error in C_* is more difficult to determine by error propagation, since C_* was calculated by a regression of concentrations and stability corrected heights for three heights (Eq. (1)). Because we found that the lowest and highest denuders have the largest contribution to the regression (Sec. 2.3), we performed the random error calculation for those two heights in analogy to Wolff et al. (2010), which can be found in Supplementary Sec. 1.2. We

obtained random errors for each half-hourly flux. As Fig. 2 shows, the average random error on a single flux value is large, varying from 60% at night to 105% during the day. However, when aggregating many fluxes, for example to calculate the mean flux or a diurnal trend, the random error decreases with $\sqrt{N}$ to small numbers.

The major source of random uncertainty for aggregated fluxes were gaps in the data (Sec. 2.3), which can be quantified by randomly introducing additional gaps. We combined all hours with valid data into one complete dataset without gaps. Next, we introduced gaps at random positions with binned gapsizes proportional to those in the original Solleveld dataset to study the impact of the additional gaps on the resulting mean flux. The standard deviation of the mean fluxes from 1000 repetitions of this procedure provided a random uncertainty of 20% in the mean ammonia flux due to gaps.

The systematic uncertainty on the GRAHAM measurements in Solleveld is unknown. In 2007, the systematic error on the concentration measurements of the GRAHAM instrument under lab conditions was quantified to be 0.6% by Wichink Kruit et al. (2007). A systematic error of 0.6% on the Solleveld concentrations would propagate to an error in the fluxes of 13%. We tried to minimize systematic uncertainties by careful inspection of the concentration measurements throughout the measurement campaign. Also, we observed that the difference between the concentrations measured by the three denuders goes to zero around noon when conditions are usually turbulent (see the diurnal trend in Supplementary Fig. S3). This supports our assumption that the systematic error on the concentrations during our measurements was small. Quadratic addition of a random uncertainty of 20% and systematic uncertainty of 13% results in a total uncertainty of 24% on the fluxes. In this paper we use an uncertainty of 24% on aggregated fluxes, such as annual means.

Furthermore, we quantified the uncertainty of the gapfilling procedure (Sec. 4.2) following a similar approach as above. We first randomly introduced gaps in a subset of the data without gaps, and then gapfilled the data to study the impact on the mean flux, like in Moffat et al. (2007). The standard deviation of 1000 repetitions of that procedure resulted in an uncertainty of 17% in the mean ammonia flux. This is smaller than the 20% uncertainty due to gaps, so our gapfilling method improved the flux estimation.

2.5. DEPAC-1D reference runs

DEPAC (DEPosition of Acidifying Compounds) is a module to calculate the surface resistance for different atmospheric compounds, like ammonia, within the commonly used resistance model analogy (Zanten et al., 2010). It is used in the Dutch suite of models (e.g. OPS (Sauter et al., 2020), LOTOS-EUROS (Manders et al., 2017) and AERIUS[1]). DEPAC calculates the effective surface resistance (which includes the compensation points for ammonia), while the aerodynamic resistance for the turbulent layer and the boundary layer resistance (R_a and R_b) are calculated in a shell around DEPAC. This so-called DEPAC-1D model can be run as a standalone model to infer ammonia fluxes on a specific site, using local concentration measurements. We have used a version of DEPAC that includes the effect of co-deposition of ammonia and sulfur dioxide (Wichink Kruit et al., 2010b, 2017).

Running the DEPAC model had a twofold function. Firstly, we wanted to improve our understanding of the exchange processes at Solleveld by qualitative comparison of measured ammonia fluxes with fluxes calculated by DEPAC. Secondly, we wanted to test how well DEPAC can model ammonia fluxes in Solleveld, because DEPAC was never parametrized for coastal dunes. We fed DEPAC with local turbulence parameters from the sonic, ammonia concentrations measured by the GRAHAM at 3.6 m height and SO$_2$ concentrations from measurement
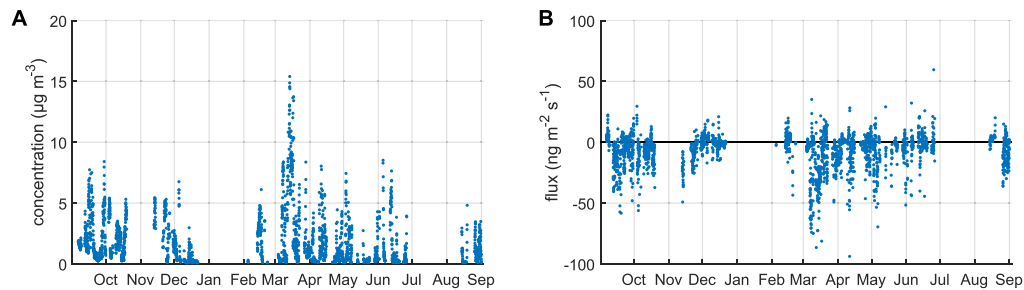
---

[1] https://www.aerius.nl/en.

Fig. 3. (A) Time series of the hourly ammonia concentration at 1 m height derived from the concentrations measured by the GRAHAM. **(B)** Time series of the hourly ammonia fluxes derived by the flux-gradient method.
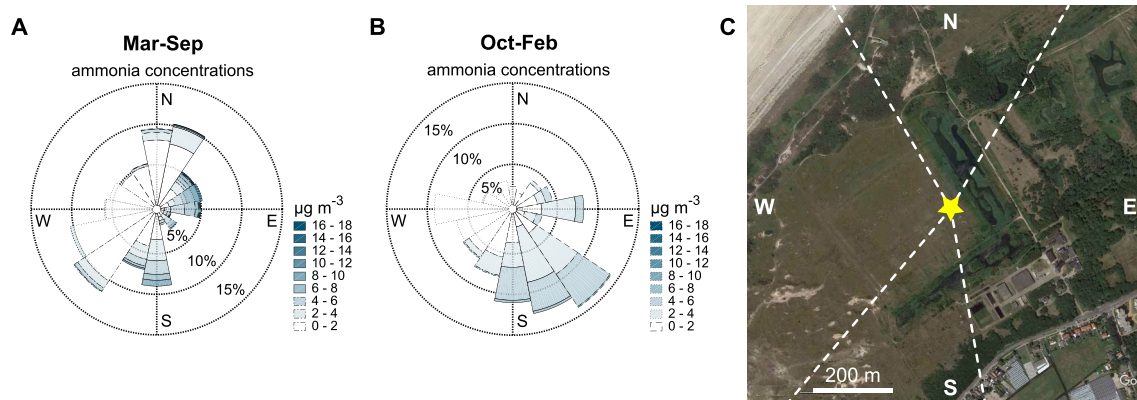

Fig. 4. (A,B) Concentration roses of the summer (A) and winter (B) season. **(C)** 1 × 1 km map of the measurement site with the location of the GRAHAM setup indicated with the yellow star. The division into four wind direction sectors is indicated by the dashed lines.

station De Zilk[2] (52°17′47.9″N, 4°30′39.0″E), which is also located in a dune ecosystem close to the North Sea coast. Furthermore, DEPAC works with hourly data, so the half-hourly ammonia concentration measurements from the GRAHAM were averaged to hourly values. For consistency, all data we show in this paper are hourly values, unless indicated otherwise.

3. Results

3.1. Time series of NH₃ concentration and flux measurements

Ammonia concentrations were measured with values mainly between 0 and 5 µg m^{-3} (Fig. 3A). Maximum concentrations up to 15.5 µg m^{-3} were found in March during manure application season. The mean and median concentrations during the measurement period were 1.9 µg m^{-3} and 1.0 µg m^{-3} respectively. Ammonia fluxes (Fig. 3B) were derived by the flux-gradient method. We observed mostly deposition, but also many emission events throughout the year. Relatively large deposition fluxes were measured in March, presumably as a result of the increased ammonia concentrations by manure application. The mean and median fluxes during the measurement period were −7.1 ± 1.7 ng m^{-2} s^{-1} and -2.9 ± 0.7 ng m^{-2} s^{-1} respectively.

3.2. Diurnal variations of concentration and flux

It is well known that seasonal effects can be observed in ammonia data (van Zanten et al., 2017), because its concentration and flux depend on parameters related to meteorology (e.g. temperature, relative humidity, rain, boundary layer height), ecosystem characteristics (e.g.

Table 1
Characteristics of the measurement data in the four quadrants shown in Fig. 4.

	North	East	South	West
Angle	330°–30°	30°–170°	170°–220°	220°–330°
Ammonia concentration	low	high	high	low
Mean calculated roughness length	0.12 m	0.12 m	0.034 m	0.010 m
Number of observations	465	913	527	868
Mean concentration	0.95 µg m^{-3}	3.9 µg m^{-3}	2.6 µg m^{-3}	0.68 µg m^{-3}

growth season of the vegetation, leaf area index, respiration properties) and agricultural practices (e.g. manure application). Therefore we divided the data into two seasons: a warmer summer/growing season from March to September and a colder winter season from October to February (Fig. 4A and B and Fig. S4). In addition, we divided the data into four wind direction sectors to account for the inhomogeneity of the measurement site (Fig. 4C). These four wind sectors are based on the average ammonia concentration and on the roughness length of the surrounding vegetation. Ammonia concentrations were higher for wind from the inland (south and east) than for wind from the sea (north and west), because most ammonia sources are located inland. The roughness length was calculated from the friction velocity and windspeed (Moene and van Dam, 2014). Vegetation in the north and east (reed, bushes, buildings) had a higher roughness length than in the south and west (mostly grass). Characteristics of the four wind quadrants can be found in Table 1.

3.2.1. Concentrations
Diurnal cycles of the mean ammonia concentrations are displayed in
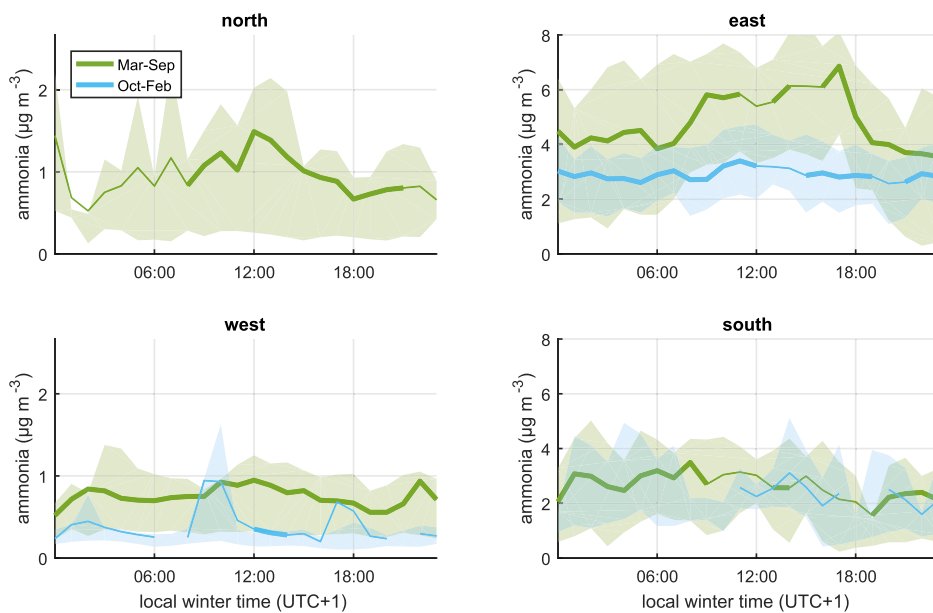
---

[2] www.luchtmeetnet.nl.

Fig. 5. Diurnal cycle of the mean ammonia concentration for the four wind sectors and two seasons. The shaded region indicates the 25/75 percentiles, and a thin/fat line means that at least 6 or 10 datapoints respectively were available. Note that the y-axis range is smaller for north and west compared to south and east. For the west one can see a very flat line in winter but with some strong deviations, caused by the availability of only few data per hour and large variability within those data, as the median (Supplementary Fig. S5) did show a flat line.
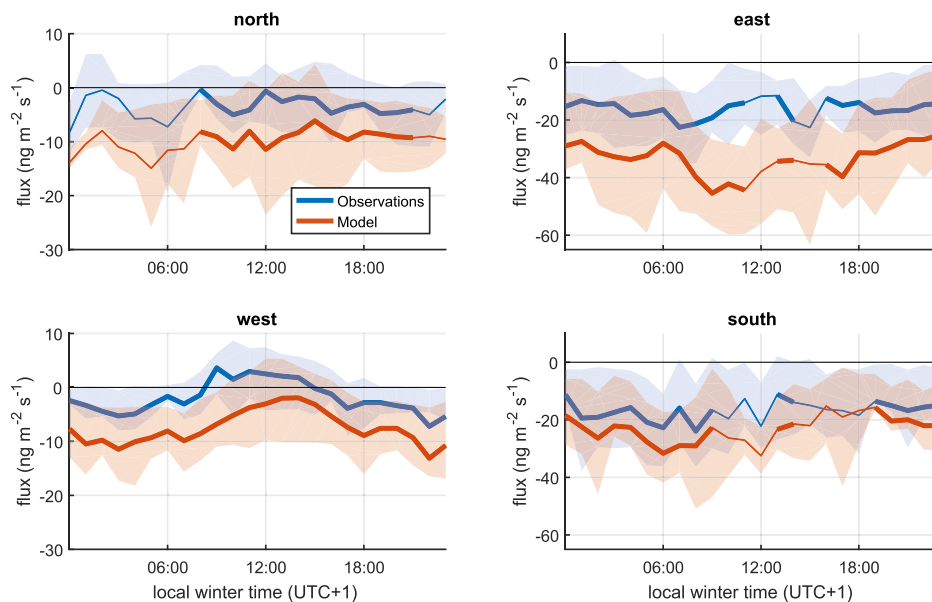

Fig. 6. Diurnal variation of the mean measured ammonia fluxes (blue) and modeled DEPAC fluxes (red) for the four wind sectors in summer. The plots for winter can be found in Fig. S7. The shaded region indicates the 25/75 percentiles, and a thin/fat line means that at least 6 or 10 datapoints respectively were available. Note that the y-axis range is smaller for north and west compared to south and east.

Fig. 5. We only included averages of hours for which at least 6 datapoints were available. A diurnal trend was only visible for wind from the east in summer. This trend was likely the result of larger emission from sources at daytime, combined with higher temperatures and lower relative humidity. For the other quadrants no clear diurnal trend could be distinguished. The pattern for north and west in Fig. 5 is caused by a few high values during midday and was as such not present in the median diurnal cycle (Fig. S5). Higher ammonia concentrations in summer compared to winter were likely the result of higher ammonia emissions (like manure application in March) and stronger evaporation of ammonia due to higher temperatures.

3.2.2. Fluxes

Fig. 6 shows the diurnal variation of the fluxes in summer, both

Table 2
Mean and median fluxes from both observations and modelling for the four wind quadrants in summer versus winter.

		North	East	South	West
Mean observed flux (ng m^{-2} s^{-1})	Summer	−3.3	−16.4	−16.9	−1.4
	Winter	–	−6.1	−6.3	−0.92
Mean DEPAC flux (ng m^{-2} s^{-1})	Summer	−9.4	−33.1	−23.5	−6.9
	Winter	–	−27.3	−20.0	−5.7

measured and modeled. The measured fluxes in Solleveld were small in general, and close to zero for wind from the sea (north and west). For wind from the west, a diurnal trend was observed with deposition at night and emission during the day. Such daytime emissions could be the
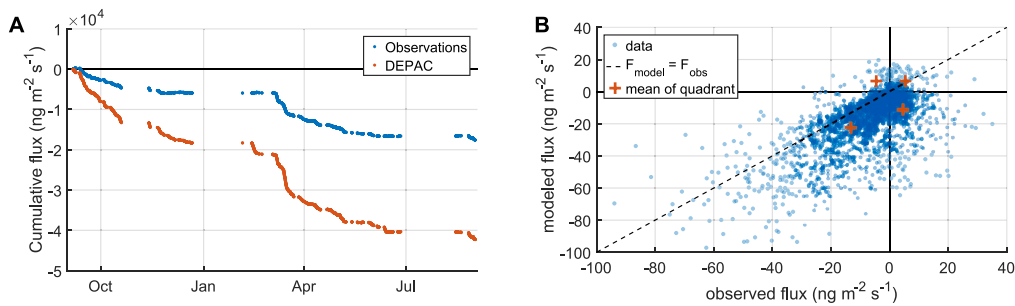
Fig. 7. (A) Comparison of the cumulative fluxes from the measurements and DEPAC model. (B) Scatterplot of the hourly DEPAC fluxes versus observed fluxes, a dashed y = x line for reference and the mean of each quadrant.

Table 3
Summary of the mean and median fluxes and the number of hours with deposition or emission fluxes from observations and DEPAC modeling.

	Observations	DEPAC
Mean flux	-7.1 ± 1.7 ng m^{-2} s^{-1}	-17.0 ng m^{-2} s^{-1}
Number of hours with deposition flux	1671	2308
Number of hours with emission flux	811	174

result of the low atmospheric ammonia concentrations (Fig. 5). When the atmospheric concentration is lower than the concentration within the canopy, net emission can take place, especially for warm and dry daytime conditions. At night, with closed stomata, higher relative humidity and lower temperatures, net deposition takes place. A diurnal trend was not so clear for wind from the other quadrants (also look at the median fluxes in Fig. S6). In winter, the measured fluxes were even closer to zero than in summer (Fig. S7 and Table 2).

3.3. Comparison of measured and modeled fluxes

In general, the shape of the observed diurnal variation in Fig. 6 was reproduced well by DEPAC, an indication that the governing ammonia

exchange processes are captured by DEPAC. The absolute value however of the modeled deposition fluxes was larger than measured. In winter, the overestimation of the fluxes was larger than in summer (Table 2). The agreement between DEPAC and measurements was best for south and west, directions with the most homogeneous vegetation (Fig. 4C). Further comparison of the modeled and measured fluxes is presented in Fig. 7 and Table 3. The mean modeled flux (-17.0 ng m^{-2} s^{-1}) was a factor 2.4 larger than the measured flux (-7.1 ng m^{-2} s^{-1}). A difference of 10 ng m^{-2} s^{-1} may not be large in absolute terms, but the modeled fluxes fall outside the uncertainty range of 24% on the measurements. Two observations from the scatterplot in Fig. 7B could explain the difference. Firstly, most points are below the $F_{model} = F_{obs}$ line, so on average DEPAC modeled larger deposition fluxes. Secondly, 811 emission events ($F_{obs} > 0$) were measured in the whole year (Table 3), while DEPAC modeled emission in only 14% of those (top-right quadrant of Fig. 7B) and deposition in the remaining 86% events (bottom-right quadrant). Following up on these observations, we performed a sensitivity analysis of certain DEPAC parameters in the next section.

3.4. Improved agreement between measurements and DEPAC

The DEPAC module for ammonia has been parametrized using measurements at the Haarweg in The Netherlands (Wichink Kruit et al.,
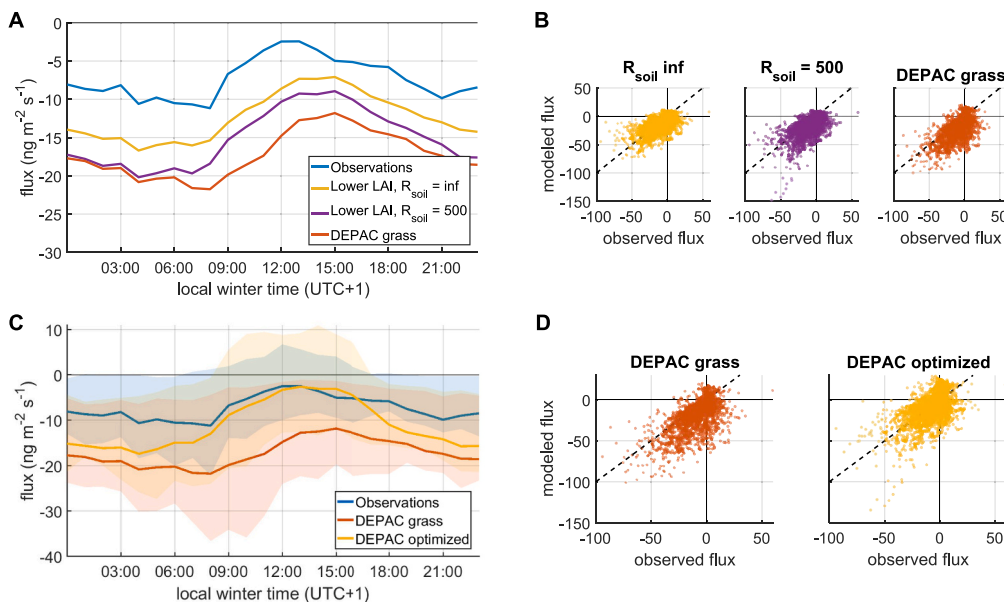

Fig. 8. (A,B) Diurnal variation (A) and scatterplots (B) of the DEPAC fluxes for standard grass settings ($LAI_{min} = 2$; $LAI_{max} = 3.5$) compared with a lower LAI ($LAI_{min} = 0.5$; $LAI_{max} = 1$), yet no exchange with the soil (yellow) and lower LAI combined with a finite soil resistance of 500 s/m (purple). (C,D) Diurnal variation with the 25/75 percentiles (C) and scatterplots of DEPAC fluxes in ng m^{-2} s^{-1} (D), both plots compare the standard grass settings in DEPAC (red) and a run with lower LAI $LAI_{min} = 0.5$; $LAI_{max} = 1.0$), $R_{soil} = 500$ s/m, $T_{min} = 1$ °C, $T_{opt} = 18$ °C, 2x higher γ_{stom} and 1.5x higher γ_w (yellow).

2010b). The vegetation at that site was predominantly temperate humid perennial ryegrass, while the main vegetation at Solleveld was sand sedge with moss and lichen. DEPAC has no separate parametrization for a dune ecosystem with such vegetation, so we used the parametrization for land use class "grass" because that most closely resembled the dune ecosystem. It seems likely that model parameters concerning ammonia exchange between vegetation and atmosphere are different at Solleveld than for ryegrass. Below, we present findings of a sensitivity study, quantifying the impact of changing the values of a limited set of DEPAC parameters on the agreement between DEPAC fluxes and observations.

The first candidate was the leaf area index (LAI). MODIS satellite LAI measurements show large variations between different vegetations (van der Graaf et al., 2020). For grass, DEPAC assumes an LAI of 2 in winter and 3.5 in summer. Inspection of the MODIS LAI values for an area around Solleveld gives lower values (between 0.5 in winter and 1.0–1.5 in summer), which is reasonable for sparse dune vegetation. Setting the LAI to lower values decreased the DEPAC fluxes (Figs. S8A and B and Table S1). As the modeled fluxes are quite sensitive to the LAI, it is important to use LAI values appropriate for the local vegetation. A lower LAI however also implies that a larger fraction of the soil surface is exposed. For grassland, we assume that the soil is fully covered with vegetation so no exchange of ammonia takes place between soil and atmosphere, which is accomplished by setting R_{inc} (in-canopy resistance) to infinity in DEPAC. One could argue that this is inappropriate for sparse canopy such as in Solleveld, so we set R_{inc} to a finite value (with $b = 14, h = 0.1$ m), and adjusted the effective soil exchange via R_{soil}. We have no measurements to determine R_{soil} for dunes, but values above 400 s/m resulted in the best match with the measured fluxes (Figs. S8C and D). One could also handle the soil exchange by adding a soil compensation point in DEPAC, but more research would be needed for that. We set $R_{soil} = 500$ s/m in combination with the lower LAI (Fig. 8A and B). This resulted in a better match with the measurements than standard grass settings, but DEPAC still modeled larger deposition fluxes than measured.

The fact that more emission events were measured than modeled (Fig. 7B) could mean that compensation points in DEPAC are too low for dune vegetation. The equations for stomatal compensation point γ_{stom} or external leaf compensation point γ_w were empirically determined using measurements above ryegrass (Wichink Kruit et al., 2010b). It is not unlikely that the constants in the equations are slightly different for other vegetation types, and a sensitivity study showed that a larger γ_{stom} or γ_w increased the number of emission events and decreases the fluxes (Figs. S8E–H and Table S1).

Another observation was that DEPAC did not model any emission fluxes for temperatures below approximately 10 °C, while we did measure emissions. DEPAC has no hard cut-off on temperature, but multiple temperature-dependent variables exist. One of them is the stomatal conductance, which becomes zero for temperatures outside a range $[T_{min}, T_{max}]$ and otherwise is multiplied with the following correction factor (Emberson et al., 2000), with T_{opt} the temperature of maximum stomatal conductance:

$$f_{temp}(T) = \frac{T - T_{min}}{T_{opt} - T_{min}} \left(\frac{T_{max} - T}{T_{max} - T_{opt}} \right)^{\frac{T_{max} - T_{opt}}{T_{opt} - T_{min}}} \tag{6}$$

We changed T_{min} from 12 °C to 1 °C and T_{opt} from 26 °C to 18 °C, which are the values of semi-natural vegetation (heather/moor) in Emberson et al. (2000). That increased the number of hours where both DEPAC and observations show emission fluxes from 117 to 286 (respectively 14% and 35% of all measured emission events). Moreover, after this adjustment, DEPAC did model emission fluxes for temperatures below 10 °C. Changing T_{min} and T_{opt} had little influence on the magnitude of the fluxes.

Combining a lower LAI ($LAI_{min} = 0.5$; $LAI_{max} = 1.0$) with finite soil path ($R_{soil} = 500$ s/m), lower T_{min} and T_{opt}, 2x higher γ_{stom} and 1.5x higher γ_w, improved the agreement between DEPAC and observations
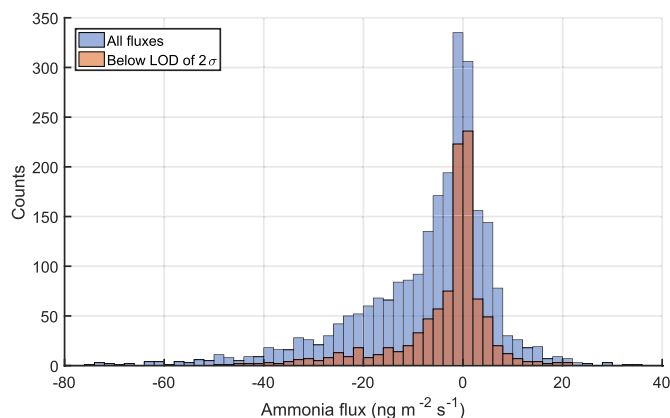

Fig. 9. Distribution of the ammonia fluxes. In blue are all measured fluxes, in red the subset that was not significantly different from zero because the concentration difference was below the LOD of 2σ.

(Fig. 8C and D). The root mean square error (RMSE) improved from 17.4 to 15.3 ng m^{-2} s^{-1} and the bias from 10.0 to 3.5 ng m^{-2} s^{-1}. Finally, the mean DEPAC flux decreased from −17.0 to −10.6 ng m^{-2} s^{-1}, much closer to the measured value of −7.1 ± 1.4 ng m^{-2} s^{-1}. During the day the agreement was better than at night, suggesting that deposition to soil or external leaf is still overestimated by the model.

In short, our analysis shows that adapting the *LAI*, R_{soil}, γ_w and γ_{stom} to values that better suit a dune vegetation can improve the agreement between measurements and DEPAC modeling. However, apart from the LAI, we have no measurements to verify whether the proposed values for aforementioned parameters are indeed better suited for dune vegetation. Also, the low data coverage of the flux measurements makes the data uncertain. Further research is thus needed to get a better estimation of the compensation points.

4. Discussion

4.1. Limit of detection

In Sec. 2.4 we discussed the random and systematic uncertainties on the ammonia fluxes. We showed that the uncertainty on a single flux value can be very large, but that the uncertainty on aggregated fluxes was determined to be 24%. Another factor of uncertainty is that the fluxes in Solleveld were very low, raising the question whether they could be distinguished from zero. The limit of detection (LOD) of an instrument is defined as 2-3σ, where σ is the precision (1.9% for the concentration measurements of the GRAHAM in field conditions (Wichink Kruit et al., 2009)). For the GRAHAM, this means that concentrations below approximately 0.1 μg m^{-3} cannot be considered significantly different from zero. Moreover, a concentration difference (and thus the flux) cannot be considered significantly different from zero when it is below 2–3x the precision of the concentration difference. For two measurement heights, that precision is easily calculated by propagation of the error on both concentrations. The GRAHAM however measured at three heights, which complicates the calculation. Because the gradient is better constrained with three heights, we chose to use the calculation as for two heights, even though that might result in a conservative estimate of the precision. We calculated a separate LOD for each hour and evaluated whether the concentration difference of the lowest and highest denuder was below the LOD (Fig. 9). In approximately 40% of the hours with valid measurements, the concentration difference was below 2σ. This means that we have to be careful looking at individual fluxes. Fortunately, when aggregating the data (for example the mean annual deposition or diurnal cycle) the limit of detection decreases with a factor $\sqrt{N}$ (Langford et al., 2015), in which case most of the measurements do make a valuable contribution to the
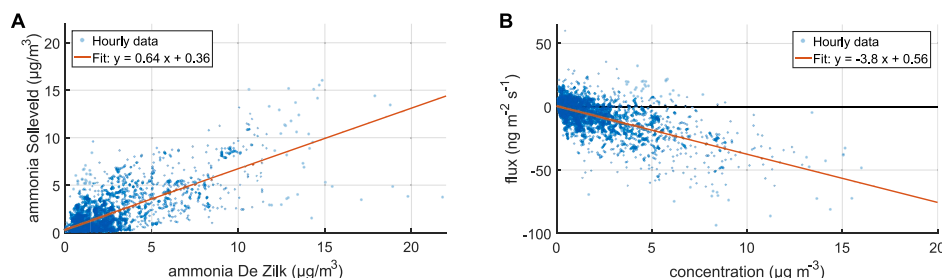
Fig. 10. (A) Scatterplot of the ammonia concentrations in Solleveld (at 3.6 m) versus those in De Zilk (3.5 m) with a linear fit. $R^2 = 0.55$ and RMSE of 2.0 μg/m^3. (B) Scatterplot of the measured ammonia flux versus the ammonia concentration (at 3.6 m) at Solleveld, $R^2 = 0.40$. This flux-concentration relation was used in combination with the gapfilled concentration series to gapfill the Solleveld fluxes.

Table 4
Comparison of the values for concentration and flux for the Solleveld dataset before and after gapfilling.

	Original data	Gapfilled data
Data coverage	28%	91%
Mean concentration	2.1 μg/m^3	1.7 μg/m^3
Median concentration	1.1 μg/m^3	1.0 μg/m^3
Mean flux	−7.1 ng/m^{2}s	−5.8 ng/m^{2}s
Median flux	−2.9 ng/m^{2}s	−4.0 ng/m^{2}s
Annual deposition flux	−160 mol N ha^{-1} yr^{-1}	−132 mol N ha^{-1} yr^{-1}

average. Therefore, concentrations and concentration differences below the LOD were not removed from the dataset (Nemitz et al., 2018).

4.2. Gapfilling

We measured hourly ammonia fluxes in Solleveld during one year with a data coverage of 28%, and found a mean ammonia flux of −7.1 ± 1.4 ng m^{-2} s^{-1}. To obtain a representative annual flux, the fluxes were gapfilled to estimate the contribution of missing datapoints. This was done by first gapfilling the ammonia concentration measurements at 3.6 m with the consistency method described by Nguyen and Hoogerbrugge (2014). Concentration data from a continuous-flow denuder ammonia monitor (AMOR) at monitoring station De Zilk were used, which is part of the Dutch National Air Quality Monitoring Network (www.luchtmeetnet.nl). De Zilk is a coastal monitoring station positioned 35 km to the north-northeast of Solleveld with a measuring height of 3.5 m. The characteristics of Solleveld and De Zilk were quite similar with mean values for overlapping periods (2215 h) of respectively 2.0 μg/m^3 and 2.6 μg/m^3, and a correlation coefficient of $R^2 = 0.55$ for hourly values (Fig. 10A). After gapfilling, the mean ammonia concentration at Solleveld was 1.7 μg/m^3 (compared to 2.1 μg/m^3 before gapfilling). The lower mean value after gapfilling was in line with the majority of missing data occurring in winter months, which commonly have lower ammonia concentrations than summer periods (Fig. 3A and Fig. S4). Next, a stochastic regression imputation was performed using the regression between Solleveld concentration and flux at 3.6 m (Fig. 10B). This relationship was applied to the gapfilled concentration data to give an estimate of the flux. Although this is a crude method ($R^2 = 0.40$), it does result in a better estimate for the annual flux. Because the mean and median fluxes were not strongly influenced by gapfilling (Table 4), we concluded that despite the limited data coverage of the GRAHAM measurements in Solleveld, we can make a robust estimate of the ammonia fluxes.

4.3. Estimation of an annual dry deposition flux for solleveld

After gapfilling, we found an annual mean dry deposition flux of −132 ± 26 mol N ha^{-1} yr^{-1}, equivalent to 1.8 ± 0.4 kg N ha^{-1} yr^{-1}, for ammonia in Solleveld. Previous estimates for nitrogen deposition in

dune ecosystems were made with inferential methods, and generally include reduced (NH$_x$) as well as oxidized (NO$_x$) nitrogen, and both wet and dry deposition. Several numbers were reported in literature. Closest to our study was a combination of wet deposition and dry inferential measurements for Solleveld (Rijkswaterstaat data repository). Those measurements provided an average N deposition over 2011–2016 of 17–22 kg N ha^{-1} yr^{-1}, of which 30% was attributed to ammonia (5–7 kg N ha^{-1} yr^{-1}). Furthermore, 6–30 kg N ha^{-1} yr^{-1} was calculated for UK sand dune sites with varying nitrogen load (Jones et al., 2004), 3–10 kg N ha^{-1} yr^{-1} around the Baltic sea (Remke, 2009), and 5–17 kg N ha^{-1} yr^{-1} in 24 sand dune locations in the UK (Field et al., 2014). Since we only measured dry deposition of ammonia, it is often hard to directly compare the numbers. However, the dry deposition of ammonia in Dutch dune areas is estimated to be about 45% of the total N deposition.[3] Applying this percentage leads to a total nitrogen deposition flux around 4 kg N ha^{-1} yr^{-1}, which falls in the low end of values reported in literature.

4.4. Comparison measurements and modeling

When comparing measured and modeled ammonia fluxes, the question arises whether it is justified to optimize the model using the measurements, which are also not 100% reliable. However, we do trust the data within the specified uncertainty range, and because the GRAHAM performance was carefully analyzed by Wichink Kruit (2010), and because the measured fluxes in Solleveld were within the range of other flux calculations in dune areas (Sec. 4.3). A model always relies on inevitable assumptions and simplifications of reality. In addition, the model is more general in contrast to the site-specific measurements, which are therefore likely to provide more reliable fluxes for the Solleveld location than DEPAC, allowing us to optimize DEPAC parameters using measured fluxes.

5. Conclusions

To investigate the dry deposition of ammonia in dune area Solleveld we measured half-hourly ammonia fluxes during one year with the aerodynamic flux-gradient method. Measurements resulted in a mean ammonia concentration of 1.9 μg m^{-3} and a mean flux of −7.1 ± 1.7 ng m^{-2} s^{-1}. We subdivided the data into two seasons and four wind direction sectors. The concentration and flux measurements in Solleveld show mostly deposition fluxes, with some (re)emission of ammonia during the day. The data coverage was about 28% due to missing data and data filtering. The data set was therefore gapfilled using nearby concentration measurements of ammonia combined with the relation between dry deposition flux and concentration derived at Solleveld. Based on the gapfilled data we found a total yearly ammonia dry deposition flux of −132 ± 32 mol ha^{-1} yr^{-1} (equivalent to 1.8 ± 0.4 kg

---

[3] Historical series GCN, available via http://www.clo.nl/nl0189.

N ha^{-1} yr^{-1}). These are small concentrations and fluxes compared to other areas in The Netherlands (Hoogerbrugge et al., 2021; Mosquera et al., 2000; Nemitz et al., 2004; COTAG dry deposition measurements, RIVM; Wichink Kruit, 2010; Wichink Kruit et al., 2010a; Wichink Kruit et al., 2007), as the Solleveld site was close to the sea and further away from ammonia sources. Furthermore, we compared measured fluxes with DEPAC modeling. DEPAC modeled 2.4x larger deposition fluxes than measured, but with a similar diurnal variation. This suggests that the governing processes are captured by DEPAC, but that certain parameters are not applicable for dune vegetation. Various model parameters were identified which can improve the match between DEPAC and measurements. Based on this analysis we propose to introduce more land use classes in DEPAC, and use satellite data to determine LAI values for those classes. We have also seen that DEPAC fluxes strongly depend on parameters such as compensation points. To check and further improve the parametrization of DEPAC for other ecosystems than grass, we recommend additional flux measurements, for example those with the new deposition DOAS setup (Swart et al. preprint; Volten et al., 2012; Wichink Kruit et al., 2010a), combined with additional measurements to determine compensation points for a dune ecosystem in analogy with Wichink Kruit et al. (2010b).

CRediT authorship contribution statement

K.J.A. Vendel: Formal analysis, Visualization, Writing – original draft, Writing – review & editing. **R.J. Wichink Kruit:** Conceptualization, Formal analysis, Methodology, Software, Writing – review & editing. **M. Blom:** Investigation, Data curation, Software. **P. van den Bulk:** Investigation, Data curation. **B. van Egmond:** Investigation, Data curation. **A. Frumau:** Formal analysis. **S. Rutledge-Jonker:** Writing – review & editing. **A. Hensen:** Conceptualization, Validation, Supervision, Writing – review & editing. **M.C. van Zanten:** Conceptualization, Funding acquisition, Formal analysis, Methodology, Software, Supervision, Writing – original draft, Writing – review & editing.

Declaration of competing interest

The authors declare that they have no known competing financial interests or personal relationships that could have appeared to influence the work reported in this paper.

Data availability

Data will be made available on request.

Acknowledgements

Appendix A. Supplementary data

Supplementary data to this article can be found online at https://doi.org/10.1016/j.atmosenv.2023.119596.

References

Aggenbach, C.J.S., Kooijman, A.M., Fujita, Y., van der Hagen, H., van Til, M., Cooper, D., Jones, L., 2017. Does atmospheric nitrogen deposition lead to greater nitrogen and carbon accumulation in coastal sand dunes? Biol. Conserv. 212, 416–422. https://doi.org/10.1016/j.biocon.2016.12.007.

Beljaars, A.C.M., Holtslag, A.A.M., 1991. Flux parameterization over land surfaces for atmospheric models. J. Appl. Meteorol. 30, 327–341. https://doi.org/10.1175/1520-0450(1991)030<0327:Fpolsf>2.0.Co;2.

Bobbink, R., Hicks, K., Galloway, J., Spranger, T., Alkemade, R., Ashmore, M., Bustamante, M., Cinderby, S., Davidson, E., Dentener, F., Emmett, B., Erisman, J.-W., Fenn, M., Gilliam, F., Nordin, A., Pardo, L., De Vries, W., 2010. Global assessment of nitrogen deposition effects on terrestrial plant diversity: a synthesis. Ecol. Appl. 20, 30–59. https://doi.org/10.1890/08-1140.1.

COTAG dry deposition measurements,RIVM. https://www.rivm.nl/stikstof/meten/droge depositieNH3.

Dyer, A.J., 1974. A review of flux-profile relationships. Boundary-Layer Meteorol 7, 363–372. https://doi.org/10.1007/BF00240838.

Emberson, L., Simpson, D., Tuovinen, J., Ashmore, M., Cambridge, H., 2000. Towards a Model of Ozone Deposition and Stomatal Uptake over Europe. MSC-W.

Erisman, J.W., Wyers, G.P., 1993. Continuous measurements of surface exchange of SO$_2$ and NH$_3$; Implications for their possible interaction in the deposition process. Atmos. Environ., Part A 27, 1937–1949. https://doi.org/10.1016/0960-1686(93)90266-2.

Field, C.D., Dise, N.B., Payne, R.J., Britton, A.J., Emmett, B.A., Helliwell, R.C., Hughes, S., Jones, L., Lees, S., Leake, J.R., 2014. The role of nitrogen deposition in widespread plant community change across semi-natural habitats. Ecosystems 17, 864–877. https://doi.org/10.1007/s10021-014-9765-5.

Finkelstein, P.L., Sims, P.F., 2001. Sampling error in eddy correlation flux measurements. J. Geophys. Res. 106, 3503. https://doi.org/10.1029/2000JD900731.

Flechard, C.R., Nemitz, E., Smith, R.I., Fowler, D., Vermeulen, A.T., Bleeker, A., Erisman, J.W., Simpson, D., Zhang, L., Tang, Y.S., Sutton, M.A., 2011. Dry deposition of reactive nitrogen to European ecosystems: a comparison of inferential models across the NitroEurope network. Atmos. Chem. Phys. 11, 2703–2728. https://doi.org/10.5194/acp-11-2703-2011.

Ford, H., Roberts, A., Jones, L., 2016. Nitrogen and phosphorus co-limitation and grazing moderate nitrogen impacts on plant growth and nutrient cycling in sand dune grassland. Sci. Total Environ. 542, 203–209. https://doi.org/10.1016/j.scitotenv.2015.10.089.

Hoogerbrugge, R., Geilenkirchen, G.P., den Hollander, H.A., Siteur, K., Smeets, W., van der Swaluw, E., de Vries, W.J., Wichink Kruit, R.J., 2021. Grootschalige concentratie- en depositiekaarten Nederland. https://doi.org/10.21945/RIVM-2021-0068. Rapportage 2021. RIVM.

Jones, M.L.M., Wallace, H.L., Norris, D., Brittain, S.A., Haria, S., Jones, R.E., Rhind, P.M., Reynolds, B.R., Emmett, B.A., 2004. Changes in vegetation and soil characteristics in coastal sand dunes along a gradient of atmospheric nitrogen deposition. Plant Biol. 6, 598–605. https://doi.org/10.1055/s-2004-821004.

Kooijman, A.M., Arens, S.M., Postema, A.E.L., van Dalen, B.R., Cammeraat, L.H., 2021. Lime-rich and Lime-Poor Coastal Dunes: Natural Blowout Activity Differs with Sensitivity to High N Deposition through Differences in P Availability to the Vegetation. Science of The Total Environment, 146461. https://doi.org/10.1016/j.scitotenv.2021.146461.

Kooijman, A.M., van Til, M., Noordijk, E., Remke, E., Kalbitz, K., 2017. Nitrogen deposition and grass encroachment in calcareous and acidic Grey dunes (H2130) in NW-Europe. Biol. Conserv. 212, 406–415. https://doi.org/10.1016/j.biocon.2016.08.009.

Langford, B., Acton, W., Ammann, C., Valach, A., Nemitz, E., 2015. Eddy-covariance data with low signal-to-noise ratio: time-lag determination, uncertainties and limit of detection. Atmos. Meas. Tech. 8, 4197–4213. https://doi.org/10.5194/amt-8-4197-2015.

Manders, A.M., Builtjes, P.J., Curier, L., Denier van der Gon, H.A., Hendriks, C., Jonkers, S., Kranenburg, R., Kuenen, J.J., Segers, A.J., Timmermans, R., 2017. Curriculum vitae of the LOTOS–EUROS (v2. 0) chemistry transport model. Geosci. Model Dev. (GMD) 10, 4145–4173. https://doi.org/10.5194/gmd-10-4145-2017.

Moene, A.F., van Dam, J.C., 2014. Transport in the Atmosphere-Vegetation-Soil Continuum. Cambridge University Press, Cambridge.

Moffat, A.M., Papale, D., Reichstein, M., Hollinger, D.Y., Richardson, A.D., Barr, A.G., Beckstein, C., Braswell, B.H., Churkina, G., Desai, A.R., Falge, E., Gove, J.H., Heimann, M., Hui, D., Jarvis, A.J., Kattge, J., Noormets, A., Stauch, V.J., 2007. Comprehensive comparison of gap-filling techniques for eddy covariance net carbon fluxes. Agric. For. Meteorol. 147, 209–232. https://doi.org/10.1016/j.agrformet.2007.08.011.

Mosquera, J., Hensen, A., Bulk, W.C.M.v.d., Vermeulen, A.T., Erisman, J.W., Möls, J.J., 2000. NH$_3$ Flux Measurements at Schagerbrug and Oostvaardersplassen, the Dutch Contribution to the GRAMINAE Experiment. ECN, p. 60.

Nemitz, E., Mammarella, I., Ibrom, A., Aurela, M., Burba, G.G., Dengel, S., Gielen, B., Grelle, A., Heinesch, B., Herbst, M., Hörtnagl, L., Klemedtsson, L., Lindroth, A., Lohila, A., McDermitt, D.K., Meier, P., Merbold, L., Nelson, D., Nicolini, G., Nilsson, M.B., Peltola, O., Rinne, J., Zahniser, M., 2018. Standardisation of Eddy-Covariance Flux Measurements of Methane and Nitrous Oxide 32, 517–549. https://doi.org/10.1515/intag-2017-0042.

Nemitz, E., Sutton, M.A., Wyers, G.P., Jongejan, P.A.C., 2004. Gas-particle interactions above a Dutch heathland: I. Surface exchange fluxes of NH$_3$, SO$_2$, HNO$_3$ and HCl. Atmos. Chem. Phys. 4, 989–1005. https://doi.org/10.5194/acp-4-989-2004.

Nguyen, P.L., Hoogerbrugge, R., 2014. Methods Used to Compensate for the Effect of Missing Data in Air Quality Measurements. National Institute for Public Health and the Environment.

Paulson, C.A., 1970. The mathematical representation of wind speed and temperature profiles in the unstable atmospheric surface layer. J. Appl. Meteorol. 9, 857–861. https://doi.org/10.1175/1520-0450(1970)009<0857:Tmrows>2.0.Co;2.

Phoenix, G.K., Emmett, B.A., Britton, A.J., Caporn, S.J., Dise, N.B., Helliwell, R., Jones, L., Leake, J.R., Leith, I.D., Sheppard, L.J., 2012. Impacts of atmospheric nitrogen deposition: responses of multiple plant and soil parameters across contrasting ecosystems in long-term field experiments. Global Change Biol. 18, 1197–1215. https://doi.org/10.1111/j.1365-2486.2011.02590.x.

Remke, E., 2009. Impact of Atmospheric Nitrogen Deposition on Lichen-Rich, Coastal Dune Grasslands. Radboud University Nijmegen, Nijmegen, PhD thesis.

Repository, Rijkswaterstaat. Waterinfo extra. https://waterinfo-extra.rws.nl/download-data/.

Sauter, F., Sterk, M., Swaluw, E.v.d., Kruit, R.W., Vries, W.d., Pul, A.v., 2020. The OPS-Model; Description of OPS 5.0.0.0. National Institute for Public Health and the Environment (RIVM), Bilthoven.

Swart, D.Z.J; van der Graaf, S;Rutledge-Jonker, S; Hensen, A; Berkhout, S; Wintjen, P; van der Hoff, R; Haaima, M; Frumau, A; van den Bulk, P; Schulte, R; van Goethem, T, In preparation. Measuring dry deposition of ammonia using flux-gradient and eddy covariance methods with two novel open-path instruments, Atmos. Meas. Tech., preprint. https://doi.org/10.5194/amt-2022-171.

Trebs, I., Ammann, C., Junk, J., 2021. Immission and dry deposition. In: Foken, T. (Ed.), Springer Handbook of Atmospheric Measurements. Springer, Cham.

van der Graaf, S.C., Kranenburg, R., Segers, A.J., Schaap, M., Erisman, J.W., 2020. Satellite-derived leaf area index and roughness length information for surface–atmosphere exchange modelling: a case study for reactive nitrogen deposition in north-western Europe using LOTOS-EUROS v2.0. Geosci. Model Dev 13, 2451–2474. https://doi.org/10.5194/gmd-13-2451-2020.

van Zanten, M.C., Wichink Kruit, R.J., Hoogerbrugge, R., Van der Swaluw, E., van Pul, W.A.J., 2017. Trends in ammonia measurements in The Netherlands over the period 1993–2014. Atmos. Environ. 148, 352–360. https://doi.org/10.1016/j.atmosenv.2016.11.007.

Volten, H., Bergwerff, J.B., Haaima, M., Lolkema, D.E., Berkhout, A.J.C., van der Hoff, G.R., Potma, C.J.M., Wichink Kruit, R.J., van Pul, W.A.J., Swart, D.P.J., 2012. Two instruments based on differential optical absorption spectroscopy (DOAS) to measure accurate ammonia concentrations in the atmosphere. Atmos. Meas. Tech. 5, 413–427. https://doi.org/10.5194/amt-5-413-2012.

Wichink Kruit, R.J., 2010. Surface-atmosphere Exchange of Ammonia - Measurements and Modeling over Non-fertilized Grassland in the Netherlands. Wageningen University, PhD thesis.

Wichink Kruit, R.J., Aben, J., de Vries, W., Sauter, F., van der Swaluw, E., van Zanten, M.C., van Pul, W.A.J., 2017. Modelling trends in ammonia in The Netherlands over the period 1990–2014. Atmos. Environ. 154, 20–30. https://doi.org/10.1016/j.atmosenv.2017.01.031.

Wichink Kruit, R.J., H, V., M, H., Dpj, S., Mc, v.Z., Waj, v.P., 2010a. Ammonia Exchange Measurements over a Corn Field in Lelystad, the Netherlands in 2009. National Institute for Public Health and the Environment, Bilthoven, The Netherlands.

Wichink Kruit, R.J., Stolk, A.P., Volten, H., Pul, W.A.J.v., RIVM, 2009. In: NH_3 Flux Measurements of Ammonia at the Micrometeorological Weather Station in Wageningen, The Netherlands. National Institute for Public Health and the Environment, p. 58.

Wichink Kruit, R.J., van Pul, W.A.J., Otjes, R.P., Hofschreuder, P., Jacobs, A.F.G., Holtslag, A.A.M., 2007. Ammonia fluxes and derived canopy compensation points over non-fertilized agricultural grassland in The Netherlands using the new gradient ammonia—high accuracy—monitor (GRAHAM). Atmos. Environ. 41, 1275–1287. https://doi.org/10.1016/j.atmosenv.2006.09.039.

Wichink Kruit, R.J., van Pul, W.A.J., Sauter, F.J., van den Broek, M., Nemitz, E., Sutton, M.A., Krol, M., Holtslag, A.A.M., 2010b. Modeling the surface–atmosphere exchange of ammonia. Atmos. Environ. 44, 945–957. https://doi.org/10.1016/j.atmosenv.2009.11.049.

Wolff, V., Trebs, I., Ammann, C., Meixner, F.X., 2010. Aerodynamic gradient measurements of the NH_3-HNO_3-NH4NO3 triad using a wet chemical instrument: an analysis of precision requirements and flux errors. Atmos. Meas. Tech. 3, 187–208. https://doi.org/10.5194/amt-3-187-2010.

Wyers, G.P., Otjes, R.P., Slanina, J., 1993. A continuous-flow denuder for the measurement of ambient concentrations and surface-exchange fluxes of ammonia. Atmos. Environ., Part A 27A, 2085–2090. https://doi.org/10.1016/0960-1686(93)90280-C.

Zanten, M.C.v., Sauter, F.J., Wichink Kruit, R.J., Jaarsveld, J.A.v., Pul, W.A.J.v., 2010. Description of the DEPAC Module. Dry Deposition Modelling with DEPAC_GCN2010. RIVM.